British Journal of Cancer

ARTICLE

Clinical Studies

APOBEC3B stratifies ovarian clear cell carcinoma with distinct immunophenotype and prognosis

Xiaoran Long[1,2,8], Huaiwu Lu[3,8], Mei-Chun Cai[1,8], Jingyu Zang[1,8], Zhuqing Zhang[1,2], Jie Wu[4], Xiaoshi Liu[1,2], Lin Cheng[1,2], Jiejun Cheng[5], Lydia W. T. Cheung[6], Zhen Shen[7], Ying Zhou[7], Wen Di[1,2]✉, Guanglei Zhuang[1,2]✉ and Xia Yin[1,2]✉

BACKGROUND: Ovarian clear cell carcinoma (OCCC) is a challenging disease due to its intrinsic chemoresistance. Immunotherapy is an emerging treatment option but currently impeded by insufficient understanding of OCCC immunophenotypes and their molecular determinants.
METHODS: Whole-genome sequencing on 23 pathologically confirmed patients was employed to depict the genomic profile of primary OCCCs. APOBEC3B expression and digital pathology-based Immunoscore were assessed by performing immunohistochemistry and correlated with clinical outcomes.
RESULTS: An APOBEC-positive (APOBEC+) subtype was identified based on the characteristic mutational signature and prevalent kataegis events. APOBEC + OCCC displayed favourable prognosis across one internal and two external patient cohorts. The improved outcome was ascribable to increased lymphocytic infiltration. Similar phenomena of APOBEC3B expression and T-cell accumulation were observed in endometriotic tissues, suggesting that APOBEC-induced mutagenesis and immunogenicity could occur early during OCCC pathogenesis. Corroborating these results, a case report was presented for an APOBEC + patient demonstrating inflamed tumour microenvironment and clinical response to immune checkpoint blockade.
CONCLUSIONS: Our findings implicate APOBEC3B as a novel mechanism of OCCC stratification with prognostic value and as a potential predictive biomarker that may inform immunotherapeutic opportunities.

British Journal of Cancer (2023) 128:2054–2062; https://doi.org/10.1038/s41416-023-02239-5

INTRODUCTION

Ovarian clear cell carcinoma (OCCC) represents a unique histological subtype of epithelial ovarian cancer (EOC). Specifically, OCCC arises from endometriosis, often endometriotic cysts on the ovary, and is more likely refractory to conventional platinum-containing chemotherapy, leading to dismal prognosis at advanced stages [1, 2]. In addition, OCCC has a characteristic genomic profile with high frequencies of *ARID1A*, *PIK3CA* and *KRAS* somatic alterations [3, 4]. At present, evidence-based treatment is lacking for OCCC, which essentially shares the same clinical practice guidelines for managing high-grade serous ovarian carcinoma (HGS-OvCa) [5]. The distinctive aetiological, clinicopathological and molecular features of OCCC underscore the necessity for implementing rational therapeutic strategies.

We have recently identified APOBEC-mediated kataegis as a notable mechanism underlying punctuated OCCC evolution [6]. While promoting neoplastic transformation and aggressiveness [7, 8], the APOBEC polynucleotide deaminases catalyse DNA mutagenesis and thereby provoke tumour immunogenicity by generating a high neoantigen load [9, 10]. Accordingly, APOBEC activity is reportedly associated with enhanced susceptibility to immune checkpoint inhibitors (ICIs) targeting programmed cell death 1 (PD-1) or programmed death ligand 1 (PD-L1) [11, 12]. Consistent with these observations, the KEYNOTE-100 and NRG-GY003 trials, among others, have implicated OCCC to potentially benefit more from ICI therapy than HGS-OvCa [13–16]. Despite the incremental progress, the interplay between APOBEC dysregulation and tumour immune microenvironment remains to be elucidated in OCCC.

Here, by expanding genome-wide analysis and including three independent patient cohorts, we further defined a molecular subtype of APOBEC-positive (APOBEC +) OCCC, marked by APOBEC mutational signature or APOBEC3B protein expression. APOBEC + OCCC showed superior prognosis and increased

[1]State Key Laboratory of Oncogenes and Related Genes, Department of Obstetrics and Gynecology, Shanghai Cancer Institute, Ren Ji Hospital, Shanghai Jiao Tong University School of Medicine, Shanghai, China. [2]Shanghai Key Laboratory of Gynecologic Oncology, Ren Ji Hospital, Shanghai Jiao Tong University School of Medicine, Shanghai, China. [3]Department of Gynecologic Oncology, Sun Yat-sen Memorial Hospital, Sun Yat-Sen University, Guangzhou, China. [4]Department of Pathology, The Affiliated Hospital of Qingdao University, Qingdao, China. [5]Department of Radiology, Ren Ji Hospital, Shanghai Jiao Tong University School of Medicine, Shanghai, China. [6]School of Biomedical Sciences, Li Ka Shing Faculty of Medicine, The University of Hong Kong, Hong Kong, China. [7]Department of Obstetrics and Gynecology, The First Affiliated Hospital of USTC, Division of Life Sciences and Medicine, University of Science and Technology of China, Hefei, China. [8]These authors contributed equally: Xiaoran Long, Huaiwu Lu, Mei-Chun Cai, Jingyu Zang. ✉email: diwen163@163.com; zhuangguanglei@gmail.com; yinxia2@aliyun.com

Received: 18 April 2022 Revised: 7 March 2023 Accepted: 16 March 2023
Published online: 30 March 2023

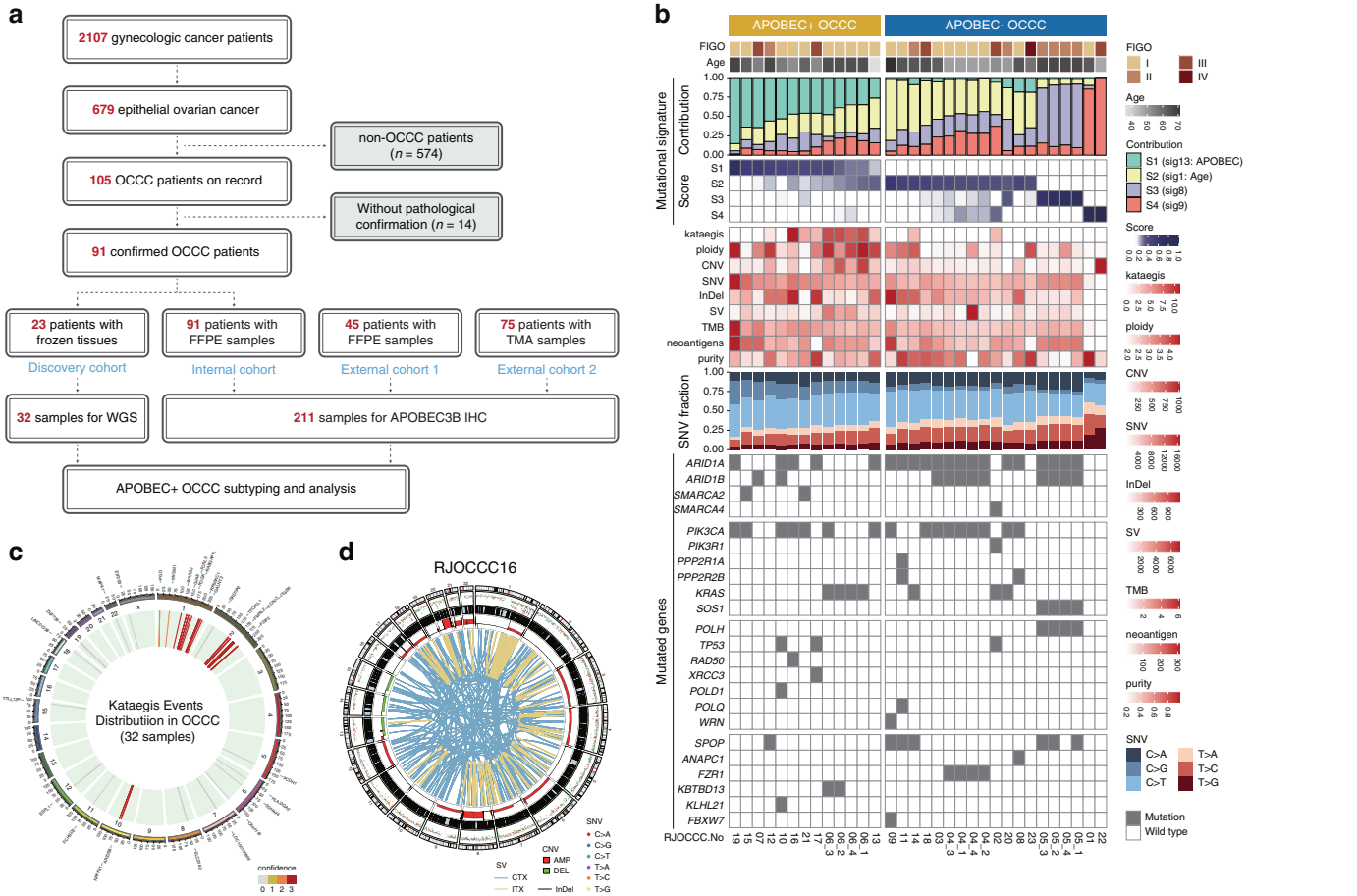

Fig. 1 WGS identifies an APOBEC + OCCC subtype. a Flowchart depicting case screening and sample analysis. The internal cohort contained 91 subjects that fulfilled the inclusion criteria. Two independent external cohorts encompassed 45 patients with FFPE tissues and 75 patients with TMA sections. **b** OncoPrint visualisation of mutational signatures, genomic features and mutational landscape derived from WGS analysis of OCCC samples. The APOBEC-related mutational signature segregated OCCC patients into two distinct molecular subtypes. **c** KataegisPortal-inferred kataegis events in sequenced OCCC samples. The circos plot summarised all kataegis loci and adjacent genes. **d** Circos plot depicting DNA sequence aberrations, copy number changes and structure variations of patient RJOCCC16. Chromosomes were arranged circularly end-to-end with rainfall plot of SNVs in the second ring and line-marked InDels in the third ring. The fourth ring displayed copy number changes. Within the inner ring each blue line denoted an interchromosomal rearrangement and each yellow line represented an intrachromosomal rearrangement. OCCC ovarian clear cell carcinoma, FFPE formalin-fixed and paraffin-embedded, TMA tissue microarray, WGS whole-genome sequencing, IHC immunohistochemistry, APOBEC+ APOBEC-positive, APOBEC− APOBEC-negative, FIGO International Federation of Gynecology and Obstetrics, CNV copy number variation, SNV single nucleotide variant, InDel insertion and deletion, SV structural variation, TMB tumour mutation burden, AMP amplification, DEL deletion, CTX interchromosomal translocations, ITX intrachromosomal translocations.

lymphocytic infiltration. Of importance, we found that an APOBEC + patient featured abundant T-cell deposit around the tumour lesion and responded exquisitely to immunotherapy treatment. Overall, these findings supported APOBEC3B as a candidate prognostic and predictive biomarker to stratify OCCC for tailored management.

RESULTS

WGS identifies an APOBEC+OCCC subtype

A comprehensive genomic and immunohistochemical study was designed for class discovery in OCCC (Fig. 1a). To this end, we retrospectively retrieved clinical records of 2107 patients diagnosed with gynaecologic cancer at Ren Ji Hospital between 2011 and 2021. Among the 679 cases of epithelial ovarian carcinoma, there were 105 OCCCs, 14 of which were excluded after pathological verification. As a result, 91 subjects fulfilled the inclusion criteria and comprised the internal OCCC cohort (Table 1). The median age was 56 years (range, 32–79 years), and disease diagnosis spanned different International Federation of Gynecology and Obstetrics stages. All patients underwent debulking surgery and the majority received one or more lines of systemic therapy. Other detailed clinicopathological and treatment information was also available (Supplementary Table 1). In parallel, two independent external cohorts were assembled including one containing 45 patients with FFPE tissues (Supplementary Table 2) and the other containing 75 patients with TMA sections (Supplementary Table 3).

Initially, a subset of OCCCs (RJOCCC1–23) in the internal cohort had fresh-frozen biospecimens (Supplementary Table 4), which were subjected to whole-genome sequencing (WGS) with multi-region sampling in three patients (RJOCCC4–6), yielding a total of 32 genomes for downstream analysis. To shed light on the mutagenic processes that shaped OCCC tumorigenesis, the SomaticSignatures framework was exploited to conduct nonnegative matrix factorisation (NMF) decomposition and extracted four mutational signatures from the whole repertoire of single nucleotide variants (SNVs) (Supplementary Fig. 1). In agreement with previous reports [6, 17–19], the APOBEC-related mutational signature was prominent and could segregate OCCC patients into two molecular subtypes (Fig. 1b), namely APOBEC + (APOBEC-positive, 10 patients) and APOBEC− (APOBEC-negative, 13

Table 1. Patient demographics of the internal cohort.

Clinicopathological characteristics	*n* = 91	Treatment and outcome	*n* = 91
Age at diagnosis, years		Surgical resection	
Median (range)	56 (32–79)	R0	84 (92.3%)
<60	55 (60.4%)	R1	7 (7.7%)
≥60	36 (39.6%)	Chemotherapy	
FIGO stage		Taxol + Cisplatin	11 (12%)
I	60 (66.0%)	Taxol + Carboplatin	71 (78%)
II	14 (15.4%)	Irinotecan + Cisplatin	1 (1.1%)
III	15 (16.5%)	None	8 (8.9%)
IV	2 (2.1%)	Systemic therapy	
ECOG score		1 line	60 (65.9%)
0	86 (94.5%)	2 or more lines	23 (25.2%)
1	5 (5.5%)	None	8 (8.9%)
Menopausal state		Immunotherapy	
Pre-menopausal	24 (26.4%)	Yes	1 (1.1%)
Post-menopausal	67 (73.6%)	No	90 (98.9%)
CA125, unit/ml		Recurrence/progression	
<35	21 (23.1%)	Yes	24 (26.4%)
≥35	70 (76.9%)	No	67 (73.6%)
CA199, unit /ml		Death	
<37	69 (75.8%)	Yes	7 (7.7%)
≥37	22 (24.2%)	No	84 (92.3%)

FIGO International Federation of Gynecology and Obstetrics, *ECOG* Eastern Cooperative Oncology Group, *R0* complete resection of all visible lesions, *R1* remaining small volume tumours of ≤1 cm.

patients). The mutation spectra and somatically mutated genes were largely analogous between the two groups (Fig. 1b). However, when assessed by KataegisPortal (Fig. 1c), APOBEC + OCCC harboured more SNVs and frequent hypermutation thunderstorms referred to as kataegis (Supplementary Fig. 2). In addition, clonal and subclonal copy number alterations involving chromosomal segments, arms or even aneuploidy were recurrently detected by Sclust (Supplementary Fig. 3). As exemplified by the circos plot of RJOCCC16 (Fig. 1d), these genomic features of APOBEC + OCCC were concordant with our formerly proposed model of catastrophic macroevolutionary leaps and might be reflective of unique biological properties.

APOBEC+OCCC shows superior prognosis

To determine the clinical utility of OCCC subtyping, we sought to probe APOBEC activity in a wider range of tumour samples with only fixed tissues that were not ideal for next-generation sequencing. The APOBEC-derived mutational signature is induced by at least one APOBEC family member [20, 21]. We and others have shown that APOBEC3B expression is relatively specific to cancer cell nucleus and impacts patient outcome in OCCC [6, 22–25]. Besides, endogenous APOBEC3B is likely the prime driver of kataegis formation [26, 27]. Therefore, APOBEC3B immunohistochemistry was performed and quantified using the H-score method (Fig. 2a), which classified OCCC cases as either positive (H-score class ≥ 1) or negative (H-score class = 0). As expected, WGS-assigned APOBEC + OCCC described above presented elevated APOBEC3B H-scores (Fig. 2b), supporting the validity of immunohistochemical assays. Building upon this proximity marker, the entire internal cohort was divided into two subgroups, also termed APOBEC + (APOBEC3B-positive, 37 patients) and APOBEC− (APOBEC3B-negative, 54 patients) to implicate presumably opposite extents of APOBEC mutagenesis. Intriguingly, APOBEC + and APOBEC − OCCC had comparable age distribution (median ages, 54 versus 56.5 years) but differed in menopausal status (pre-menopausal patients, 30% versus 5%). Of note, a substantial proportion of APOBEC + OCCC appeared before menopause (Fig. 2c), implying its earlier tumour onset than APOBEC − OCCC. More importantly, APOBEC3B stratified patients into prognostically significant categories. Notably, APOBEC + OCCC exhibited prolonged progression-free survival (PFS) and overall survival (OS) as compared with APOBEC − OCCC (Fig. 2d), irrespective of disease stages (Supplementary Fig. 4A). Corroborating these data, similar observations were made in two external cohorts with either FFPE (Fig. 2e; Supplementary Fig. 4B) or TMA (Fig. 2f; Supplementary Fig. 4C) specimens. Hence, we concluded that APOBEC + OCCC showed superior prognosis over APOBEC − OCCC.

APOBEC + OCCC has increased lymphocytic infiltration

Considering the role of APOBEC enzymes in fuelling genetic diversity [8, 28], we reasoned that the favourable outcome of APOBEC + OCCC could be attributed to its immunoreactive characteristics. The OCCC immune microenvironment has been scarcely investigated other than occasional description of low and heterogeneous lymphocytic infiltrates [16, 29]. We set out to evaluate tumour-infiltrating lymphocytes by staining CD3 + pan T cells and CD8 + cytotoxic T cells (Fig. 3a). Remarkably, APOBEC3B protein expression was associated with a more inflamed immunophenotype manifested by increased T-cell recruitment (Fig. 3b). Given that APOBEC deregulation probably occurred early based on the pseudo-timeline estimation with TrackSig (Supplementary Fig. 5), APOBEC3B, CD3 and CD8 were also stained in endometriosis (Fig. 3c), the well-established precursor lesion of OCCC, and the same tendency as seen in neoplasms was evident (Fig. 3d). To analyse OCCC immune contexture more rigorously, we employed the digital pathology-based Immunoscore system (Fig. 3e), a prognostic biomarker tool validated extensively in colorectal cancer [30–32]. By capturing the densities of CD3 + and CD8 + lymphocytes at the invasive margin (IM) and the core of the tumour (CT), OCCCs were categorised as Immunoscore + (Immunoscore ≥ 1) or Immunoscore− (Immunoscore = 0) (Fig. 3f). Confirming prior results, APOBEC + OCCC was disproportionally enriched for Immunoscore

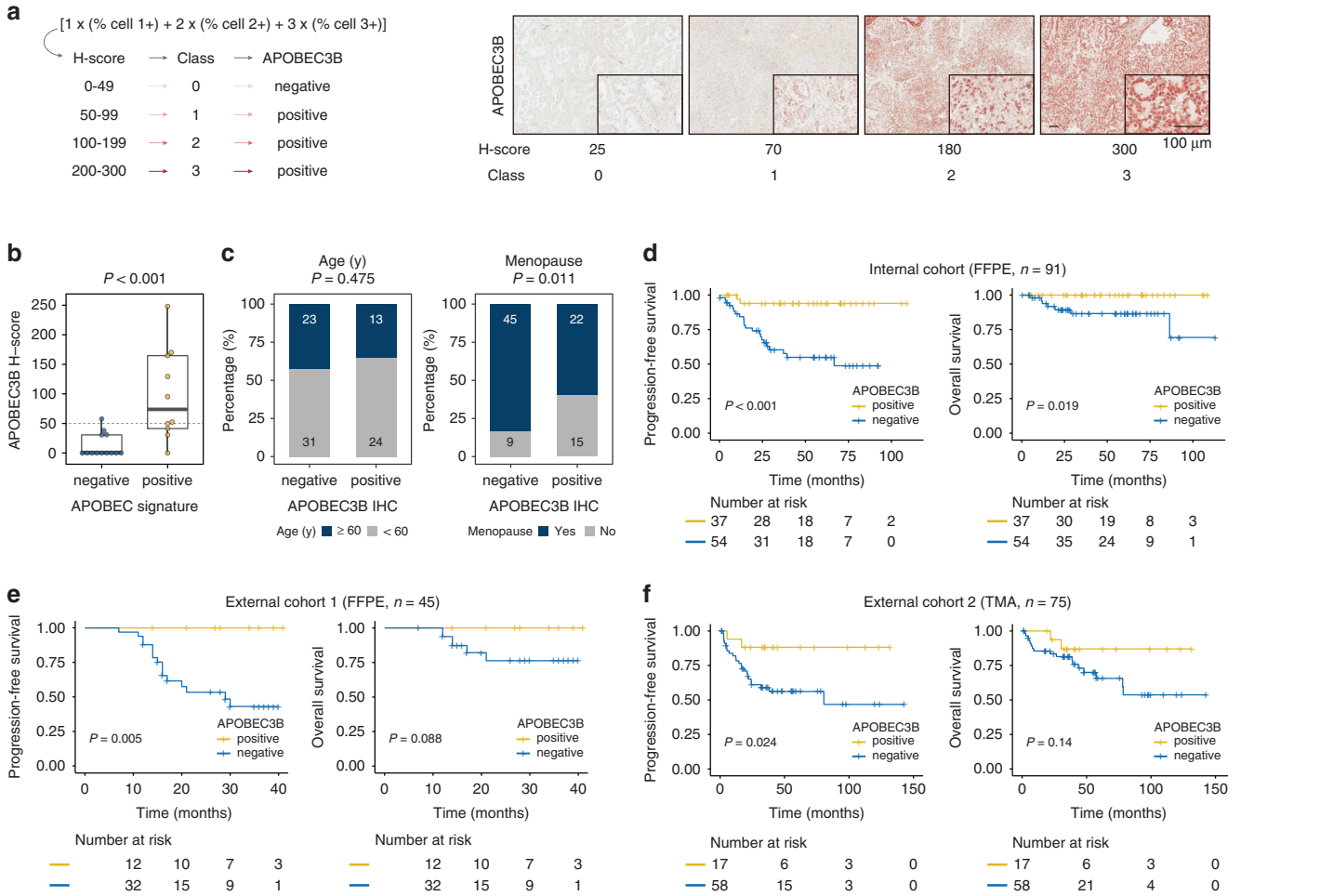

Fig. 2 APOBEC + OCCC shows superior prognosis. a A schematic illustration of the H-score method to quantify APOBEC3B staining. Representative immunohistochemical images were shown with corresponding H-scores and class labels. **b** Box plot comparing APOBEC3B H-scores in APOBEC + OCCC and APOBEC − OCCC. **c** Stacked bar plot showing the percentage of patients with the indicated demographics (age or menopause) in APOBEC + OCCC and APOBEC − OCCC. **d** Kaplan–Meier plots illustrating associations between APOBEC3B expression and progression-free or overall survival in the internal cohort. **e** Kaplan–Meier plots illustrating associations between APOBEC3B expression and progression-free or overall survival in the external cohort 1. **f** Kaplan–Meier plots illustrating associations between APOBEC3B expression and progression-free or overall survival in the external cohort 2.

+ samples in both internal and external cohorts (Fig. 3g). As a key checkpoint protein, PD-L1 expression was assess in parallel using a standardised immunohistochemical assay (Supplementary Fig. 6A) and only showed a marginal overlap with APOBEC3B positivity (Supplementary Fig. 6B), highlighting the advantage of Immunoscore method. Therefore, APOBEC + OCCC was immunologically active and accompanied by a higher degree of lymphocytic infiltration.

Immune density and localisation impact patient survival

Since Immunoscore was documented as a key parameter linked with the evolution and fate of various cancers [33], we explored the prognostic impact of immune cell densities in OCCC. While the performance of PD-L1 expression was relatively poor (Supplementary Fig. 6C), we found positive Immunoscore to be associated with beneficial clinical outcome including improved PFS and OS in the internal patient cohort (Fig. 4a; Supplementary Fig. 7A). Consistently, Immunoscore+ status in the external OCCC cohort demonstrated a statistically significant correlation with prolonged PFS and a nonsignificant trend to longer OS (Fig. 4b; Supplementary Fig. 7B), possibly due to limited sample size or inadequate death events. Recently, three immunophenotypes reflecting both T-cell quantity and spatial distribution were introduced [34]. Following such definition, Immunoscore− OCCCs were tentatively termed 'immune-desert', and Immunoscore+ OCCCs were further specified into 'immune-excluded' or 'immune-infiltrated' according to the peritumoral or intratumoral patterns of T cell infiltration, respectively (Fig. 4c). Kaplan–Meier analysis indicated that 'immune-desert' OCCC had relatively shorter PFS and OS than 'immune-infiltrated' OCCC, and 'immune-excluded' OCCC displayed intermediate risk of disease progression (Fig. 4d; Supplementary Fig. 7C). Taken together, the magnitude and topology of baseline lymphocytic infiltrates aided OCCC stratification with prognostic relevance.

APOBEC+OCCC may benefit from immunotherapy

Finally, we reported a case study of immunotherapy treatment in an OCCC patient to reinforce the potential therapeutic value of our findings. This 56-year-old female was diagnosed with FIGO stage IIB OCCC in May 2019. Pathological examination after radical surgery revealed that her tumour belonged to the APOBEC + subtype with an Immunoscore of 2 (Fig. 5a). Unfortunately, she was intolerant to the first-line paclitaxel-carboplatin regimen and suffered early recurrence of multiple pelvic lesions within ~6 months (Fig. 5b). The patient did not respond to the second-line chemotherapy (liposomal doxorubicin) either and thus elected to receive off-label use of concurrent toripalimab (anti-PD-1) to address the progressive disease. Upon three cycles

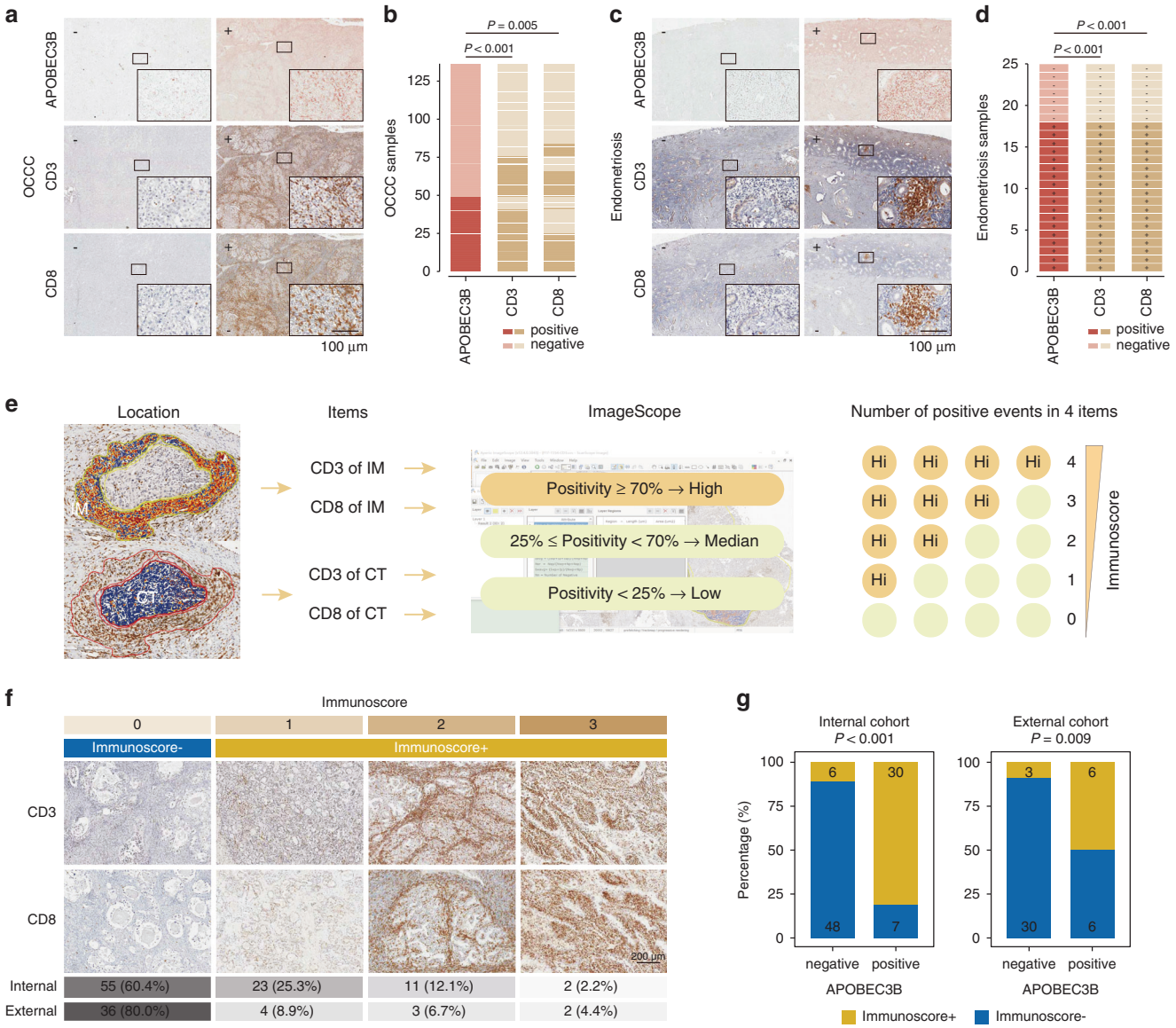

Fig. 3 APOBEC + OCCC has increased lymphocytic infiltration. a Representative immunohistochemical images of APOBEC3B, CD3 and CD8 for OCCC samples. **b** Heatmap illustrating the relationship of APOBEC3B, CD3 and CD8 status in OCCC samples. **c** Representative immunohistochemical images of APOBEC3B, CD3 and CD8 for endometriosis specimens. **d** Heatmap illustrating the relationship of APOBEC3B, CD3 and CD8 status in endometriosis specimens. **e** A schematic illustration of the digital pathology-based Immunoscore algorithm. **f** Representative immunohistochemical images for each Immunoscore were shown with corresponding percentages of OCCC patients in the internal or external cohort. **g** Stacked bar plot showing the percentage of Immunoscore+ samples in APOBEC + OCCC and APOBEC − OCCC. APOBEC + OCCC was disproportionally enriched for Immunoscore+ samples in both internal and external cohorts.

of toripalimab administration, all nascent nodules experienced extensive tumour regression at radiographic measurement. Consequently, she was able to undergo secondary cytoreduction with complete resection followed by maintenance immunotherapy, and by far remained relapse-free as evaluated by magnetic resonance imaging (MRI) with a PFS-2 of over 18 months. Based on these encouraging preliminary data, whether APOBEC3B and Immunoscore could serve as predictive biomarkers for ICIs should be tested in future investigations.

DISCUSSION

To our knowledge, this work represents one of the most systematic characterisations of OCCC mutational landscape at the genome-wide scale. The results not only confirm the punctuated model of OCCC evolution [6], but also pinpoint a unique molecular subtype linked to APOBEC-mediated mutagenesis. We provide immunohistochemical methods to stratify a large series of OCCC samples in three independent cohorts by APOBEC3B positivity and to delineate the OCCC immunophenotypes based on Immunoscore status. APOBEC + OCCC has proved to be associated with marked lymphocytic infiltration and prolonged patient survival. The possibly far-reaching therapeutic implications are upheld by robust response to immune checkpoint blockade in a case study of APOBEC + OCCC. These findings may enhance OCCC prognostication and biomarker-driven treatment to improve clinical decision-making and ultimate outcome of this otherwise devastating disease.

We and others have unveiled that APOBEC-related mutational signature is common and functionally important in both OCCC and endometriotic epithelium [6, 17–19, 35]. It has been well recognised that APOBEC-catalysed aberrant cytosine deamination leads to

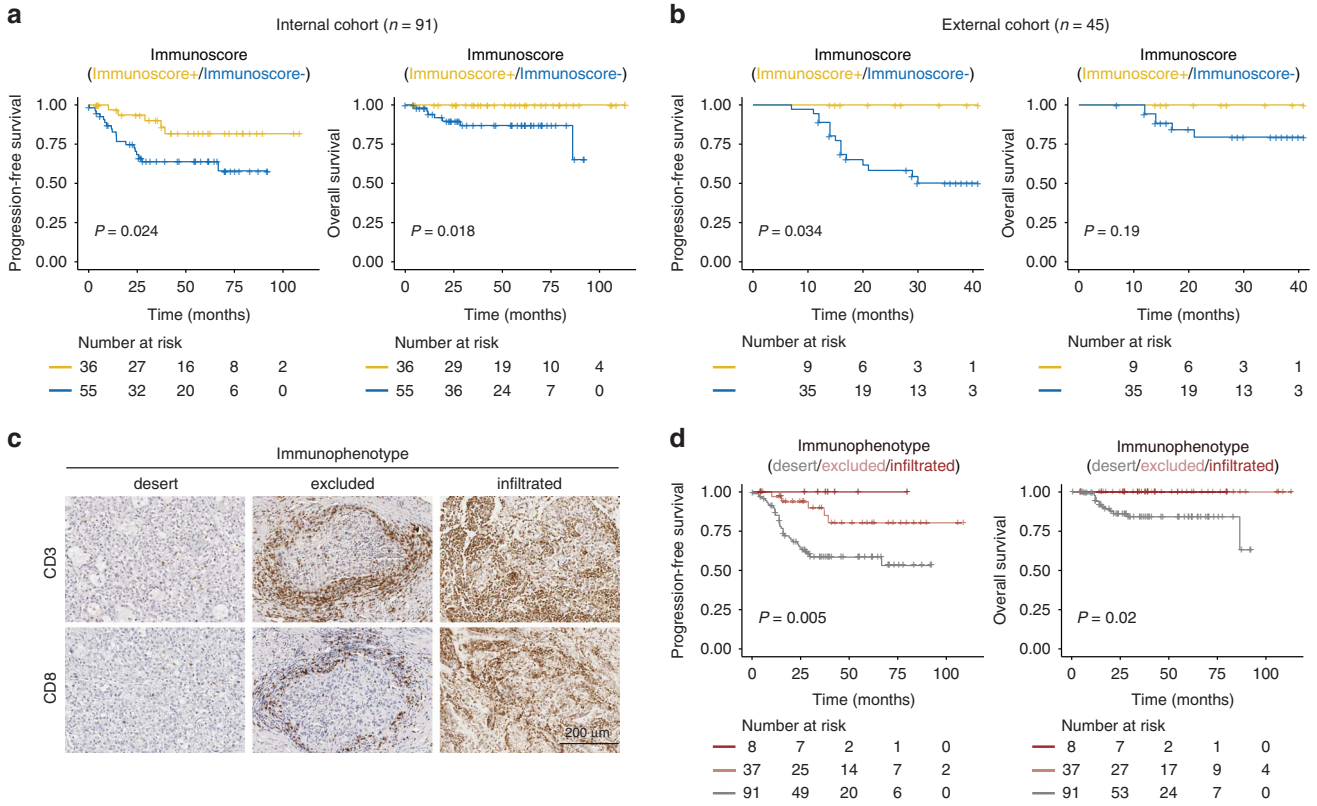

Fig. 4 Immune density and localisation impact patient survival. a Kaplan–Meier plots illustrating associations between Immunoscore and progression-free or overall survival in the internal cohort. **b** Kaplan–Meier plots illustrating associations between Immunoscore and progression-free or overall survival in the external cohort. **c** Representative immunohistochemical images of CD3 and CD8 for each of the three immunophenotypes, namely 'immune-desert', 'immune-excluded' and 'immune-infiltrated'. **d** Kaplan–Meier plots illustrating associations between immunophenotypes and progression-free or overall survival in the combined cohort of internal and external patients.

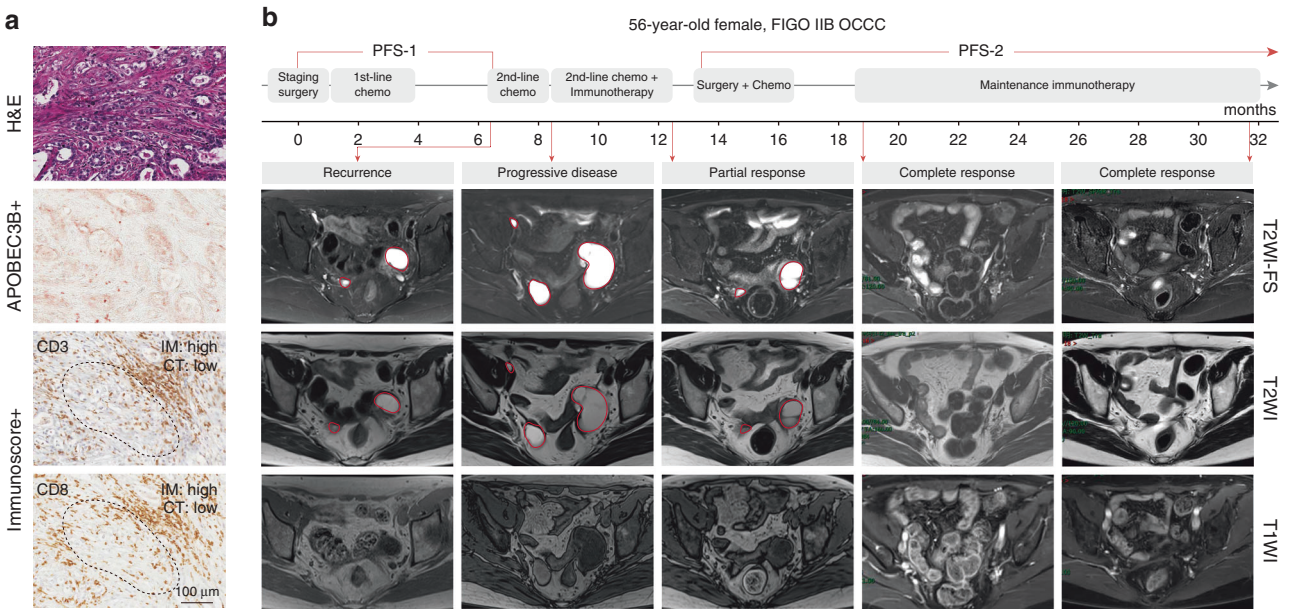

Fig. 5 APOBEC + OCCC may benefit from immunotherapy. a Immunohistochemical images of APOBEC3B, CD3 and CD8 for a pathologically confirmed OCCC patient. The tumour belonged to the APOBEC + subtype with an Immunoscore of 2. **b** Timeline of the treatment course and serial magnetic resonance imaging for the selected OCCC patient. All lesions progressed while on second-line chemotherapy, and experienced extensive tumour regression upon toripalimab administration. H&E hematoxylin and eosin, IM invasive margin, CT core of the tumour, FIGO International Federation of Gynecology and Obstetrics, OCCC ovarian clear cell carcinoma, PFS progression-free survival, T2WI-FS fat-suppressed T2-weighted image, T2WI T2-weighted image, T1WI T1-weighted image.

chromosomal instability and genetic heterogeneity, which can accelerate cancer initiation and evolution [7]. Indeed, we found that APOBEC3B protein expression and resultant kataegis events were detectable at different stages of OCCC development. The lack of high-quality antibodies has exacerbated the challenge of assessing other APOBEC paralogs, which is to be tackled in the future. Furthermore, the molecular underpinnings of APOBEC dysregulation during OCCC pathogenesis are currently elusive. Our genomic analysis indicated that APOBEC activation was unlikely modulated by specific mutant gene products. Given the pivotal role of APOBEC enzymes in viral restriction, it is tempting to hypothesise that APOBEC activity is stimulated by the inflammatory pathways such as PKC/NF-κB and interferon signalling [36, 37]. Alternatively, oestrogen exposure, tumour hypoxia, somatic retrotransposition and replication stress are all candidate instigating factors [38–41]. It is worth noting that these diverse mechanisms are not necessarily mutually exclusive and may operate successively or simultaneously to facilitate the APOBEC-induced mutator phenotype. In line with this notion, recent evidence has highlighted the episodic rather than consistent nature of APOBEC mutagenic process [40]. Additional research is required to fully understand the mechanistic basis and biological significance of APOBEC mobilisation in the context of OCCC tumorigenesis.

We leveraged APOBEC signature or APOBEC3B immunostaining to segregate OCCC patients into two distinct classes. Of particular note, in contrast to some reports of other cancer types [42], APOBEC + OCCC exhibited better prognosis in comparison with APOBEC − OCCC across internal and external cohorts. As a matter of fact, only two individuals (stages, IC and IIB) out of 37 APOBEC + OCCC cases relapsed and neither of them died during the follow-up period (durations, 12 and 26 months), whereas 22 out of 54 APOBEC− OCCC patients progressed with 7 deaths at our centre. We applied the semiquantitative Immunoscore algorithm to categorise OCCC for the first time, and demonstrated that higher levels of in situ immune infiltrates could, at least in part, accounted for the longer survival durations of APOBEC + OCCC. As the enzymatic source of elevated mutation rate, APOBEC family members also cause collateral DNA damage and neoantigen formation in host tumour cells, resulting in vigorous immunogenicity [9, 10]. Therefore, the above-mentioned favourable outcome as a consequence of APOBEC deregulation seems counterintuitive but not surprising. Another plausible explanation has been proposed that APOBEC3B-imposed genotoxic stress sensitises malignant cells to platinum inhibition [25]. In either scenario, since adjuvant chemotherapy in stage I OCCC is under debate [43], we envision that APOBEC-dependent molecular subtyping, upon prospective evaluation, holds enormous promise for more tailored strategies to optimise the benefit-risk balance.

Despite intensive endeavours for improvement, OCCC is hitherto in urgent need of new therapeutic modalities owing to its innate chemoresistance, especially in the recurrent setting [2]. Our finding from TrackSig inference that APOBEC-associated mutagenesis can operate and impart evolutionary advantages throughout the disease course of a certain OCCC subpopulation, reminiscent of previous observations in various cancers [8], raises the appealing possibility of pharmacologically blocking APOBEC3B for targeted intervention. Along this line, immense efforts have been undertaken in drug discovery of specific small-molecules against APOBEC deaminases [44]. An alternative avenue to be pursued is APOBEC-dictated synthetic lethality with selected anticancer agents such as ATR and UNG inhibitors [23, 42, 45, 46]. In addition, encouraged by the initial efficacy signals [13–16], there is an increasing interest in treating OCCC patients with immunotherapy, and a number of ICI regimens are being actively investigated in ongoing clinical trials [43, 47, 48]. Nevertheless, the overall response rate to is still low and we now report preliminary evidence that APOBEC3B is a potential discriminant biomarker for optimal responders, which warrants further exploration with larger OCCC samples. Moreover, it should be fascinating to know whether chemical manipulation of APOBEC expression or activity by agonistic compounds to induce genomic hypermutation will augment tumour immunity and confer ICI responsiveness [28]. In view of these considerations, we argue that both APOBEC antagonism and agonism are recommended to be assessed in OCCC, depending on different treatment strategies.

Several limitations have to be acknowledged. First, although the use of three independent OCCC cohorts represents a strength of our work, one major weakness is the retrospective nature of collected samples with varied follow-up duration and scarce application of immunotherapy. Apparently, prospective studies need to be undertaken for validating APOBEC-based molecular subtyping as a prognostic and predictive biomarker. Second, only APOBEC3B is primarily analysed due to its prominent role in driving mutagenesis and kataegis formation. Ideally, all APOBEC family members ought to be comprehensively surveyed. Third, despite being cost-effective and easy to implement for routine pathology, the Immunoscore system simply relies on the densities of CD3 + and CD8 + lymphocytes from a snapshot to describe immunophenotypes, which may underestimate the contribution of spatial heteterogeneity and other components within tumour immune microenvironment. Finally, considering the wide breadth of APOBEC3B expression beyond OCCC [22, 49], it would be desirable to determine if the concepts presented here are broadly applicable to a variety of human malignancies.

MATERIALS AND METHODS

Patient cohorts

The study was approved by the Ethics Committee of Ren Ji Hospital. All patients were consented to Institutional Review Board-approved protocols. Among the 2107 gynaecologic cancer patients who were treated at the Department of Obstetrics and Gynecology, Ren Ji Hospital, 679 patients with epithelial ovarian cancer were retained for further analyses. Their clinical records were retrospectively retrieved, and there were 105 cases of ovarian clear cell carcinoma (OCCC) on record, 14 of which were excluded after pathological confirmation. In total, 91 subjects comprised the internal OCCC cohort. For the external validation cohorts, we enroled 45 and 72 patients from Sun Yat-Sen Memorial Hospital and the Affiliated Hospital of Qingdao University, respectively. Detailed clinicopathological characteristics of the three patient cohorts were described in Supplementary Tables. Fresh-frozen tumour tissues were collected during debulking surgery. Formalin-fixed and paraffin-embedded (FFPE) sections were obtained in pathologic examination. Magnetic resonance imaging (MRI) data were provided by the Department of Radiology, Ren Ji Hospital.

Whole-genome sequencing and data analysis

A total of 32 samples from 23 treatment-naïve patients (RJOCCC1–23) were subjected to whole-genome sequencing (WGS) on an Illumina HiSeq X Ten platform. WGS data of six patients (RJOCCC1–6) were recently presented and reanalysed in this study. Sequence alignment and analysis were processed as previously described [6]. Briefly, Paired-end clean reads were aligned to the human reference genome (UCSC hg19) using Burrows-Wheeler Aligner [50]. Single-nucleotide variants (SNVs) and small insertions and deletions (INDELs) were called using MuTect and Strelka [51, 52], respectively. ANNOVAR was used to annotate somatic alterations [53]. Copy number, purity and ploidy estimates were computed by Sclust [54]. CREST was implemented to identify potential structural variants [55]. Kataegis analysis was performed using KataegisPortal R package [6]. For mutational signature extraction, SNVs were analysed by nonnegative matrix factorisation (NMF) decomposition with SomaticSignatures [56]. TrackSig was used to estimate the evolutionary trajectories of mutational signatures [57]. Circular layout of genomic information was generated using circlize R package [58]. The sequencing data have been deposited in NCBI SRA database under the accession number SRP157148.

Neoantigen prediction

To predict the neoantigens in silico, nonsynonymous SNVs served as basis to generate a list of peptides ranging 8–14 amino acids in length with the mutated residues represented in each position. Polysolver was used for inference of class I HLA alleles [59]. Prediction for binding affinity of every

mutant peptide and its corresponding wild-type peptide to the patient's germline HLA alleles was performed using the NetMHCpan algorithm (v4.0) [60]. Candidate neoantigens were defined as those with a predicted mutant peptide binding affinity below 500 nM and less than that of its corresponding wild-type peptide.

Immunohistochemistry

Immunohistochemistry (IHC) was performed on 5 μm thick FFPE sections or tissue microarray (TMA). After dewaxing and hydration, the slides were treated for antigen heat repair within sodium citrate solution for 20 min. The slides were then treated for 10 min with 3% H_2O_2 in methanol to quench endogenous peroxidase activity, blocked with goat serum, incubated with primary antibodies against CD3 (Kit-0003, MXB biotechnologies) or CD8 (RMA-0514, MXB biotechnologies) at 4 °C overnight, and subjected to incubation with horseradish peroxidase (HRP) conjugated secondary antibody for 1 h at room temperature. Antigen visualisation was performed using 3,3′-diaminobenzidine (DAB) chromogen (Vector Laboratories). Slides were counterstained with hematoxylin, dehydrated and cover slipped with mounting solution (Invitrogen). For APOBEC3B staining, after deparaffinization, rehydration, antigen retrieval and protein blocking, the slides were incubated with an APOBEC3B antibody (LS-A11154, Lifespan Biosciences) for 1 h at room temperature. Thereafter, the slides were incubated with HRP-conjugated secondary antibody for 30 min at room temperature. HRP detection was performed by using aminoethyl carbazole (AEC) as substrate according to the manufacturer's protocol (AR1020, Boster Bio). Finally, slides were mounted with aqueous mounting medium (AR1018, Boster Bio). The PD-L1 staining was performed on an Autostainer Link 48 system (Agilent) with a diagnostic PD-L1 antibody (Clone 22C3, Dako). Whole slides were scanned at ×20× magnification with an Aperio ScanScope system (Leica Biosystems).

IHC staining quantification

The APOBEC3B staining was quantified using the H-score method. The H-score was calculated by adding the percentage of positive cells multiplied by an ordinal value corresponding to the intensity level (none = 0, weak = 1, moderate = 2, strong = 3). H-scores ranged from 0 to 300, and tissue samples with H-scores of ≥50 points were considered positive. The Immunoscore was a computer-assisted image assay based on the quantification of CD3 + and CD8 + lymphocytes at the invasive margin (IM) and the core of the tumour (CT). In the three-category analysis, a 0–25% density was classified as 'low', a 25–70% density was classified as 'intermediate', and a 70–100% density was classified as 'high'. The four percentiles (two markers, two regions) were calculated and converted into the Immunoscore system, with one 'high' grade scored as 1 point. A tumour was considered Immunoscore− if its Immunoscore = 0. A tumour was considered Immunoscore+ if its Immunoscore ≥ 1. The PD-L1 staining was quantified using combined positive score (CPS), i.e. the number of PD-L1-positive cells (tumour cells, lymphocytes, macrophages) divided by the number of viable tumour cells, multiplied by 100. A tumour was considered PD-L1 + if its CPS ≥ 1.

Statistical analysis

Statistics and graphics were generated using GraphPad Prism (v8.0) or R (v4.1.0). Cumulative survival rate was calculated by the Kaplan–Meier method and different groups were compared by means of log-rank tests. Statistical analysis for comparison of continuous variables including H-scores was performed using unpaired Student's *t*-tests. Chi-square tests were used to compare categorical variables, such as differences in patient demographics and tumour characteristics between APOBEC + and APOBEC − OCCC. All tests were two-sided and *P*-values of <0.05 were considered statistically significant.

DATA AVAILABILITY

The sequencing data generated in this study have been deposited in NCBI SRA database under the accession number SRP157148. All the other data and materials are available within the article or upon request from the corresponding authors.

REFERENCES

1. Karnezis AN, Cho KR, Gilks CB, Pearce CL, Huntsman DG. The disparate origins of ovarian cancers: pathogenesis and prevention strategies. Nat Rev Cancer. 2017;17:65–74.
2. Iida Y, Okamoto A, Hollis RL, Gourley C, Herrington CS. Clear cell carcinoma of the ovary: a clinical and molecular perspective. Int J Gynecol Cancer. 2021;31:605–16.
3. Khalique S, Lord CJ, Banerjee S, Natrajan R. Translational genomics of ovarian clear cell carcinoma. Semin Cancer Biol. 2020;61:121–31.
4. Itamochi H, Oishi T, Oumi N, Takeuchi S, Yoshihara K, Mikami M, et al. Whole-genome sequencing revealed novel prognostic biomarkers and promising targets for therapy of ovarian clear cell carcinoma. Br J Cancer. 2017;117:717–24.
5. Armstrong DK, Alvarez RD, Bakkum-Gamez JN, Barroilhet L, Behbakht K, Berchuck A, et al. Ovarian Cancer, Version 2.2020, NCCN Clinical Practice Guidelines in Oncology. J Natl Compr Cancer Netw. 2021;19:191–226.
6. Yin X, Bi R, Ma P, Zhang S, Zhang Y, Sun Y, et al. Multiregion whole-genome sequencing depicts intratumour heterogeneity and punctuated evolution in ovarian clear cell carcinoma. J Med Genet. 2020;57:605–9.
7. Venkatesan S, Angelova M, Puttick C, Zhai H, Caswell DR, Lu WT, et al. Induction of APOBEC3 exacerbates DNA replication stress and chromosomal instability in early breast and lung cancer evolution. Cancer Discov. 2021;11:2456–73.
8. Swanton C, McGranahan N, Starrett GJ, Harris RS. APOBEC enzymes: mutagenic fuel for cancer evolution and heterogeneity. Cancer Discov. 2015;5:704–12.
9. Smid M, Rodriguez-Gonzalez FG, Sieuwerts AM, Salgado R, Prager-Van der Smissen WJ, Vlugt-Daane MV, et al. Breast cancer genome and transcriptome integration implicates specific mutational signatures with immune cell infiltration. Nat Commun. 2016;7:12910.
10. Driscoll CB, Schuelke MR, Kottke T, Thompson JM, Wongthida P, Tonne JM, et al. APOBEC3B-mediated corruption of the tumor cell immunopeptidome induces heteroclitic neoepitopes for cancer immunotherapy. Nat Commun. 2020;11:790.
11. Wang S, Jia M, He Z, Liu XS. APOBEC3B and APOBEC mutational signature as potential predictive markers for immunotherapy response in non-small cell lung cancer. Oncogene. 2018;37:3924–36.
12. Miao D, Margolis CA, Vokes NI, Liu D, Taylor-Weiner A, Wankowicz SM, et al. Genomic correlates of response to immune checkpoint blockade in microsatellite-stable solid tumors. Nat Genet. 2018;50:1271–81.
13. Matulonis UA, Shapira-Frommer R, Santin AD, Lisyanskaya AS, Pignata S, Vergote I, et al. Antitumor activity and safety of pembrolizumab in patients with advanced recurrent ovarian cancer: results from the phase II KEYNOTE-100 study. Ann Oncol. 2019;30:1080–7.
14. Zamarin D, Burger RA, Sill MW, Powell DJ Jr., Lankes HA, Feldman MD, et al. Randomized phase II trial of nivolumab versus nivolumab and ipilimumab for recurrent or persistent ovarian cancer: an NRG Oncology Study. J Clin Oncol. 2020;38:1814–23.
15. Hamanishi J, Mandai M, Ikeda T, Minami M, Kawaguchi A, Murayama T, et al. Safety and antitumor activity of anti-PD-1 antibody, nivolumab, in patients with platinum-resistant ovarian cancer. J Clin Oncol. 2015;33:4015–22.
16. Howitt BE, Strickland KC, Sholl LM, Rodig S, Ritterhouse LL, Chowdhury D, et al. Clear cell ovarian cancers with microsatellite instability: a unique subset of ovarian cancers with increased tumor-infiltrating lymphocytes and PD-1/PD-L1 expression. Oncoimmunology. 2017;6:e1277308.
17. Wang YK, Bashashati A, Anglesio MS, Cochrane DR, Grewal DS, Ha G, et al. Genomic consequences of aberrant DNA repair mechanisms stratify ovarian cancer histotypes. Nat Genet. 2017;49:856–65.
18. Shibuya Y, Tokunaga H, Saito S, Shimokawa K, Katsuoka F, Bin L, et al. Identification of somatic genetic alterations in ovarian clear cell carcinoma with next generation sequencing. Genes Chromosomes Cancer. 2018;57:51–60.
19. Oliveira D, Schnack TH, Poulsen TS, Christiansen AP, Hogdall CK, Hogdall EV. Genomic sub-classification of ovarian clear cell carcinoma revealed by distinct mutational signatures. Cancers (Basel). 2021;13:5242.
20. Pecori R, Di Giorgio S, Paulo Lorenzo J, Nina Papavasiliou F. Functions and consequences of AID/APOBEC-mediated DNA and RNA deamination. Nat Rev Genet. 2022;23:505–18.
21. Salter JD, Bennett RP, Smith HC. The APOBEC protein family: united by structure, divergent in function. Trends Biochem Sci. 2016;41:578–94.
22. Burns MB, Temiz NA, Harris RS. Evidence for APOBEC3B mutagenesis in multiple human cancers. Nat Genet. 2013;45:977–83.
23. Green AM, Weitzman MD. The spectrum of APOBEC3 activity: from anti-viral agents to anti-cancer opportunities. DNA Repair (Amst). 2019;83:102700.
24. Ng JCF, Quist J, Grigoriadis A, Malim MH, Fraternali F. Pan-cancer transcriptomic analysis dissects immune and proliferative functions of APOBEC3 cytidine deaminases. Nucleic Acids Res. 2019;47:1178–94.
25. Serebrenik AA, Argyris PP, Jarvis MC, Brown WL, Bazzaro M, Vogel RI, et al. The DNA cytosine deaminase APOBEC3B is a molecular determinant of platinum responsiveness in clear cell ovarian cancer. Clin Cancer Res. 2020;26:3397–407.
26. Maciejowski J, Chatzipli A, Dananberg A, Chu K, Toufektchan E, Klimczak LJ, et al. APOBEC3-dependent kataegis and TREX1-driven chromothripsis during telomere crisis. Nat Genet. 2020;52:884–90.
27. Consortium ITP-CAoWG. Pan-cancer analysis of whole genomes. Nature. 2020;578:82–93.
28. Vile RG, Melcher A, Pandha H, Harrington KJ, Pulido JS. APOBEC and cancer viroimmunotherapy: thinking the unthinkable. Clin Cancer Res. 2021;27:3280–90.

29. Khalique S, Nash S, Mansfield D, Wampfler J, Attygale A, Vroobel K, et al. Quantitative assessment and prognostic associations of the immune landscape in ovarian clear cell carcinoma. Cancers (Basel). 2021;13:3854.
30. Galon J, Mlecnik B, Bindea G, Angell HK, Berger A, Lagorce C, et al. Towards the introduction of the 'Immunoscore' in the classification of malignant tumours. J Pathol. 2014;232:199–209.
31. Pages F, Mlecnik B, Marliot F, Bindea G, Ou FS, Bifulco C, et al. International validation of the consensus Immunoscore for the classification of colon cancer: a prognostic and accuracy study. Lancet. 2018;391:2128–39.
32. Angell HK, Bruni D, Barrett JC, Herbst R, Galon J. The immunoscore: colon cancer and beyond. Clin Cancer Res. 2020;26:332–9.
33. Bruni D, Angell HK, Galon J. The immune contexture and Immunoscore in cancer prognosis and therapeutic efficacy. Nat Rev Cancer. 2020;20:662–80.
34. Hegde PS, Karanikas V, Evers S. The where, the when, and the how of immune monitoring for cancer immunotherapies in the era of checkpoint inhibition. Clin Cancer Res. 2016;22:1865–74.
35. Revathidevi S, Nakaoka H, Suda K, Fujito N, Munirajan AK, Yoshihara K, et al. APOBEC mediated mutagenesis drives genomic heterogeneity in endometriosis. J Hum Genet. 2022;67:323–9.
36. Leonard B, McCann JL, Starrett GJ, Kosyakovsky L, Luengas EM, Molan AM, et al. The PKC/NF-kappaB signaling pathway induces APOBEC3B expression in multiple human cancers. Cancer Res. 2015;75:4538–47.
37. Roper N, Gao S, Maity TK, Banday AR, Zhang X, Venugopalan A, et al. APOBEC mutagenesis and copy-number alterations are drivers of proteogenomic tumor evolution and heterogeneity in metastatic thoracic tumors. Cell Rep. 2019;26:2651–66 e2656.
38. Udquim KI, Zettelmeyer C, Banday AR, Lin SH, Prokunina-Olsson L. APOBEC3B expression in breast cancer cell lines and tumors depends on the estrogen receptor status. Carcinogenesis. 2020;41:1030–7.
39. Bader SB, Ma TS, Simpson CJ, Liang J, Maezono SEB, Olcina MM, et al. Replication catastrophe induced by cyclic hypoxia leads to increased APOBEC3B activity. Nucleic Acids Res. 2021;49:7492–506.
40. Petljak M, Alexandrov LB, Brammeld JS, Price S, Wedge DC, Grossmann S, et al. Characterizing mutational signatures in human cancer cell lines reveals episodic APOBEC mutagenesis. Cell. 2019;176:1282–94 e1220.
41. Kanu N, Cerone MA, Goh G, Zalmas LP, Bartkova J, Dietzen M, et al. DNA replication stress mediates APOBEC3 family mutagenesis in breast cancer. Genome Biol. 2016;17:185.
42. Petljak M, Maciejowski J. Molecular origins of APOBEC-associated mutations in cancer. DNA Repair (Amst). 2020;94:102905.
43. Gadducci A, Multinu F, Cosio S, Carinelli S, Ghioni M, Aletti GD. Clear cell carcinoma of the ovary: epidemiology, pathological and biological features, treatment options and clinical outcomes. Gynecol Oncol. 2021;162:741–50.
44. Grillo MJ, Jones KFM, Carpenter MA, Harris RS, Harki DA. The current toolbox for APOBEC drug discovery. Trends Pharm Sci. 2022;43:362–77.
45. Buisson R, Lawrence MS, Benes CH, Zou L. APOBEC3A and APOBEC3B activities render cancer cells susceptible to ATR inhibition. Cancer Res. 2017;77:4567–78.
46. Serebrenik AA, Starrett GJ, Leenen S, Jarvis MC, Shaban NM, Salamango DJ, et al. The deaminase APOBEC3B triggers the death of cells lacking uracil DNA glycosylase. Proc Natl Acad Sci USA. 2019;116:22158–63.
47. Ngoi NY, Heong V, Ow S, Chay WY, Kim HS, Choi CH, et al. A multicenter phase II randomized trial of durvalumab (MEDI-4736) versus physician's choice chemotherapy in recurrent ovarian clear cell adenocarcinoma (MOCCA). Int J Gynecol Cancer. 2020;30:1239–42.
48. Oda K, Hamanishi J, Matsuo K, Hasegawa K. Genomics to immunotherapy of ovarian clear cell carcinoma: Unique opportunities for management. Gynecol Oncol. 2018;151:381–9.
49. Roberts SA, Lawrence MS, Klimczak LJ, Grimm SA, Fargo D, Stojanov P, et al. An APOBEC cytidine deaminase mutagenesis pattern is widespread in human cancers. Nat Genet. 2013;45:970–6.
50. Li H, Durbin R. Fast and accurate short read alignment with Burrows-Wheeler transform. Bioinformatics. 2009;25:1754–60.
51. Cibulskis K, Lawrence MS, Carter SL, Sivachenko A, Jaffe D, Sougnez C, et al. Sensitive detection of somatic point mutations in impure and heterogeneous cancer samples. Nat Biotechnol. 2013;31:213–9.
52. Saunders CT, Wong WS, Swamy S, Becq J, Murray LJ, Cheetham RK. Strelka: accurate somatic small-variant calling from sequenced tumor-normal sample pairs. Bioinformatics. 2012;28:1811–7.
53. Wang K, Li M, Hakonarson H. ANNOVAR: functional annotation of genetic variants from high-throughput sequencing data. Nucleic Acids Res. 2010;38:e164.
54. Cun Y, Yang TP, Achter V, Lang U, Peifer M. Copy-number analysis and inference of subclonal populations in cancer genomes using Sclust. Nat Protoc. 2018;13:1488–501.
55. Wang J, Mullighan CG, Easton J, Roberts S, Heatley SL, Ma J, et al. CREST maps somatic structural variation in cancer genomes with base-pair resolution. Nat Methods. 2011;8:652–4.
56. Gehring JS, Fischer B, Lawrence M, Huber W. SomaticSignatures: inferring mutational signatures from single-nucleotide variants. Bioinformatics. 2015;31:3673–5.
57. Rubanova Y, Shi R, Harrigan CF, Li R, Wintersinger J, Sahin N, et al. Reconstructing evolutionary trajectories of mutation signature activities in cancer using TrackSig. Nat Commun. 2020;11:731.
58. Gu Z, Gu L, Eils R, Schlesner M, Brors B. circlize Implements and enhances circular visualization in R. Bioinformatics. 2014;30:2811–2.
59. Shukla SA, Rooney MS, Rajasagi M, Tiao G, Dixon PM, Lawrence MS, et al. Comprehensive analysis of cancer-associated somatic mutations in class I HLA genes. Nat Biotechnol. 2015;33:1152–8.
60. Jurtz V, Paul S, Andreatta M, Marcatili P, Peters B, Nielsen M. NetMHCpan-4.0: improved peptide-MHC class I interaction predictions integrating eluted ligand and peptide binding affinity data. J Immunol. 2017;199:3360–8.

ACKNOWLEDGEMENTS

Not applicable.

AUTHOR CONTRIBUTIONS

XY, GZ and WD designed and supervised the study. XL, HL, JZ, ZZ, JW, XL, LC, JC, LWTC, ZS and YZ performed the experiments and analysed the data. MCC developed the bioinformatics pipeline. GZ and XL wrote the manuscript. All authors read and approved the final version of the manuscript.

FUNDING

This work was supported by the National Natural Science Foundation of China (82173077 and 82211540402 to XY; 81922047 and 82172596 to GZ; 81974454 to WD; 82022078 to LC), National Key Research and Development Program of China (2021YFC2700400 to WD), Shanghai Municipal Education Commission-Gaofeng Clinical Medicine Grant Support (20161313 to GZ), Shanghai Natural Science Foundation (20ZR1433100 to XY), Shanghai Shenkang Hospital Development Center (SHDC2020CR3057B to XY; SHDC2020CR6009-002 to WD), Shanghai Municipal Key Clinical Specialty, Shanghai Collaborative Innovation Center for Translational Medicine (TM202004 to XY), Beijing Kuanghua foundation for the development of Chinese and Western Medicine (BKF) (KH-2021-LLZX-018 to XY; KH-2021-LLZX-049 to HL), Shanghai Jiao Tong University School of Medicine (YG2021GD02 and TMSK-2021-207 to XY), innovative research team of high-level local universities in Shanghai (SHSMU-ZLCX20210200 to GZ), and 111project (no. B21024 to GZ).

COMPETING INTERESTS

The authors declare no competing interests.

ETHICS APPROVAL AND CONSENT TO PARTICIPATE

The study protocols were reviewed and approved by the institutional ethics committee of Ren Ji Hospital, Shanghai Jiao Tong University School of Medicine (approval number: 2018-114). Written informed consent was obtained from all the patients.

ADDITIONAL INFORMATION

Supplementary information The online version contains supplementary material available at https://doi.org/10.1038/s41416-023-02239-5.

Correspondence and requests for materials should be addressed to Wen Di, Guanglei Zhuang or Xia Yin.